Special Topic paper on an experimental technique:

Electron Energy Loss Spectroscopy (EELS)

Zihan XU (A53044451), UCSD

1. Introduction

Electron energy loss spectroscopy (EELS), just as its name suggests, measures the energy differences of transmitted electrons due to their interactions with the estimated sample. Although EELS deals with the energy loss, there is still a zero loss peak, corresponding to the elastic scattering events. The ideal EELS spectrum is shown in Figure 1, which contains the zero loss peaks, plasmon resonance, and higher loss part, including the atom core-loss peak and fine structures.

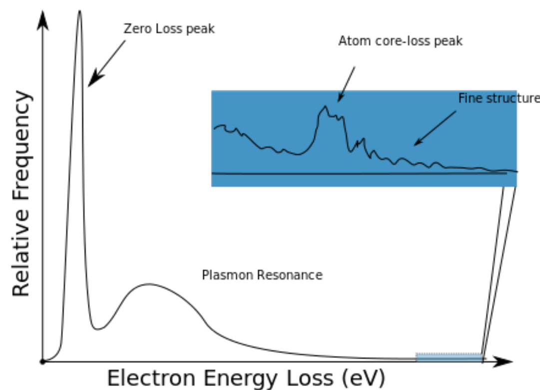

Fig 1. Ideal EELS Spectrum

2. History

As an experiential technique currently widely used in probing chemical, electrical and optical properties of a material, EELS actually appeared as early as 1940s. However, only after the development and improvement of vacuum technology and microscope instrumentation for about half a century, could EELS be useful in both solving real material problems and developing model systems.

3. Classification

According to the incident beam energy level, EELS can be classified into high-resolution electron energy-loss spectroscopy (HREELS), Reflection energy-loss spectroscopy (REELS), and the typical TEM/STEM EELS. HREELS has a incident electron beam with 100–1000 eV, and deals with small energy losses (10^{-3} –1 eV), which is a useful tool in surface science, studying the adsorption, valence electron

excitation and vibrational modes of surface atoms. When we increase the input e-beam energy, the interaction will no longer be confined within several atoms layers. If the electrons reach the surface at a glancing angle, they will still be scattered out, penetrating only several thin layers. That is the case for REELS, which has an initial energy of 100 keV at least.

When we want to investigate more about the inside properties of the specimen, we need to ensure that the electrons arrive perpendicularly at the surface with enough energies, as well as the specimen is thin enough associated with the input energy. In this way, the electrons can transmit the material, which is the TEM-EELS. TEM-EELS can be subdivided into valence EELS (from plasmon excitation and inter/intra-band transitions, from low loss spectrum) and inner-shell ionization EELS (from high loss spectrum).

4. Instrumentation

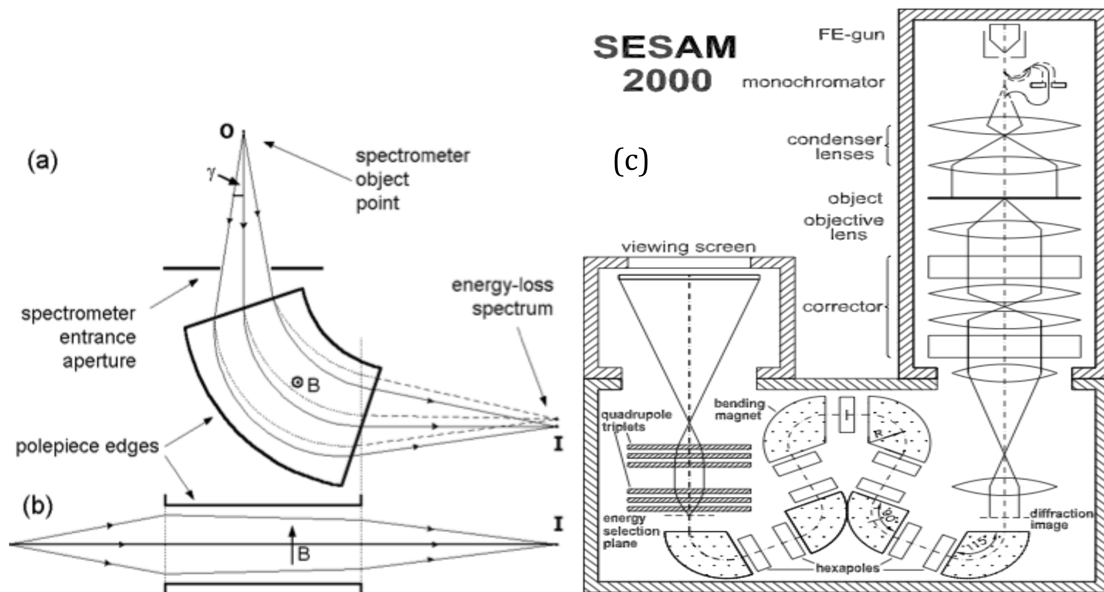

Fig 2. (a, b) Dispersive and focusing properties of a magnetic prism
(c) lens system of electron monochromator

The magnetic prism, in Figure2 (a b), is a very important part of TEM-EELS. It bends the electrons according to their energies. Within the uniform magnetic field B, electrons follow circular paths of radius R and change an angle of 90 degree. Solid lines in Figure 2 (a, b) represent zero-loss electrons (E = 0); dashed lines represent those that have lost energy. And we have: $R = (m/e)(1/B)v$ (1).

Among the three procedures for TEM-based energy-loss spectroscopy in Figure3: (a) conventional TEM with a magnetic-prism spectrometer below the viewing screen, (b) TEM incorporating an in-column imaging filter and (c) scanning-transmission (STEM) system, I'd like to discuss a bit more about the third one based on STEM, which is used in my reference paper. The dark-field stands for the electrons scattered with a large angle, while the spectrometer records the transmitted electrons with relatively small angles. The input signal is from a display device scanned in synchronism with the probe scanning to a ring-shaped detector. We could obtain the spectrum at each probe position from the serial mode.

The aberrations of the electron spectrometer could affect the energy resolution. And inserting an electron monochromator (like Fig 2(c)) after the electron source, can also improve it.

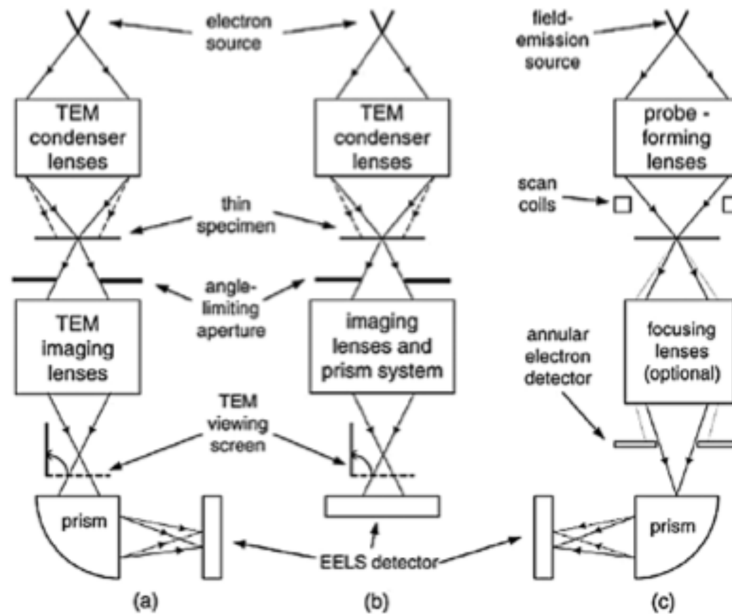

Fig. 3. 3 procedures for TEM-based energy-loss spectroscopy

5. Physics Principles

When the electrons travel through the specimen, it could have elastic and inelastic scattering. The elastic scattered electrons can affect the route of inelastic scattered ones and they generally interact with the atomic nucleus.

For ***elastic scattering*** by a single atom, the probability of scattering per unit solid angle Ω is: $d\sigma_e/d\Omega=[4Z^2/(k_0{}^2T)](\theta^2+\theta_0{}^2)^{-2}$. (2)

Z is the atomic number, k0 is the electron wavenumber (2π/wavelength) and T is an incident energy given by: $T = m_0 v_0^2/2 = E_0[1 + E_0/(2m_0c^2)]/[1 + E_0/(m_0c^2)]$ (3)

Elastic scattering brings an energy transfer E given by : $E = E_{max} \sin^2 (\theta /2)$. (4)

For ***inelastic scattering***, the double-differential cross section is given by a small-angle approximation:

$$d^2\sigma_i/d\Omega\, dE = (4\gamma^2/q^2)(R/E)(df/dE) = (4a_0^2R^2/T)[(1/E)(df/dE)](\theta^2 + \theta_E^2)^{-1} \quad (5)$$

where q is the magnitude of the scattering wavevector, $a_0 = 53 \times 10^{-12}$ m, R = 13.6 eV (the Rydberg energy), characteristic angle $\theta_E = E/(2\gamma T)$, $q = k_0(\theta + \theta_E)$.

We could get $q_{min}/q_p = c/v$ (6), where q_p is for photon adsorption and q_{min} is for electron scattering (θ=0). The incident-electron energy is more than 100keV ($v/c \approx 0.55$) and we ensure spectrometer entrance aperture with angles small enough ($\beta \ll \theta_E$) so that the transferred momentum is only about twice larger than for photon absorption. In this way, the EELS spectrum can present optical (direct) electronic transitions that obey a dipole sum rule: ($\Delta l = \pm 1$). The E-dependence df/dE is dependent on the specimen, which makes EELS useful.

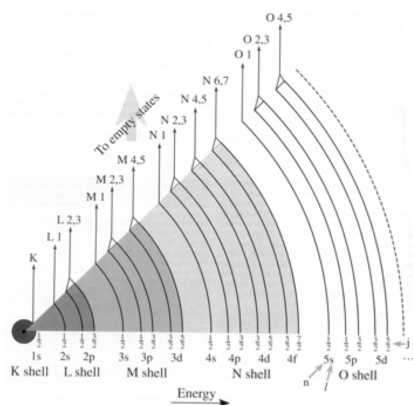

The phonon and plasmon excitations, inner shell ionizations, inter and intra band transitions and Cherenkov radiation can lead to inelastic scattering. We are usually interested in the inner-shell edges and the near-edge fine structure (ELNES) and the extended energy-loss fine structure (EXELFS). And the core-loss intensity $J_c(E)$ (i.e. spectral intensity minus pre-edge background) is given by the Fermi golden rule:

$J_c(E) \propto d\sigma_c/dE \propto M(E)^2N(E) \propto (df/dE)N(E)$ (7) , where M(E) is an atomic matrix element, df/dE is the atomic oscillator strength, and N(E) is the density of final states in the electron transition. The core-loss fine structure shows the density of unoccupied states above the Fermi level.

Chemical Shift can also happen in EELS, when there are changes in the chemical environment of an atom, which is about several eV shift in the threshold energy of an ionization edge. Because the core electron's final state is just between the Fermi level and the vacuum level, the chemical shift will also affect the valence-band width,

showing information about the occupied states. By integrating the core-loss intensity over a proper energy window, we could get the sharp ionization edges for element analysis such as the chemical shift.

6. Discussion of the Reference Paper(ref 10)

In my reference paper, *Scanning transmission electron microscopy investigation of the Si(111)/AlN interface grown by metalorganic vapor phase epitaxy*, the author takes advantage of Electron Energy Loss Spectroscopy(EELS) to study the Si(111)/AlN interface at a sub-nanometer scale. Their data were acquired on a FEI-Titan 80-300 cubed electron microscope operated at 300 keV and equipped with an aberration corrector of the probe-forming lens, an electron beam monochromator, an aberration corrector of the imaging lens, and a Gatan model 866 imaging filter.

Because Si, Al, N are all light elements, they get high-angle annular dark field (HAADF) of the interface with a 75 mrad ADF inner angle as shown in Figure 4(a, b). And they investigate the same area in annular bright field (ABF) with a 12–26 mrad detector, shown in Figure 4(d), to have a better visibility of the lighter N. Although the existence of amorphous interface (the black area in Fig4-a&b), we could see the AlN and Si still grow in certain directions. We could also see in another paper, shown in Figure 7, using ABF to illustrate the position of lighter element (O column locations, compared with Ti and Sr), for the signal scale of HAADF in STEM strongly related to the atomic numbers. That is why we need to normalize the intensity for Figure 5.

In Figures5b-d, there are the Si, N, and Al maps obtained from the spectrum-image with reference spectra acquired in the same conditions, by multiple linear least squares fit. It is easy to extract the N-K edge (401 eV), but a bit difficult to extract the L_{23} edges, which are overlapped for Si (99 eV) and Al (77 eV). Figure 5(e) is the EELS profiles obtained by integrating the signal perpendicularly to the interface. We could tell from Figure 5 that the interface corresponds to a SiN_x layer, and Si even extends to the AlN layer.

In Figure 6, we show the ELNES of the Si-L_{23}, Al-L_{23}, and N-K edges. There is a chemical shift between bulk Si and Si of the interface (2.5 ± 0.5 eV), indicating the change of filled states of electrons of Si, which is about the Si-N bonding in the amorphous phase. And further, we could conclude that the predeposition of Al couldn't forbid the reactions between Si and N and the formation of SiNx layer is the first step of growth progress. From EELS spectrum, we could tell that the interface is

not only about the disorder of crystals but also the diffusion of Si atoms, moreover, those Si atoms form strong bonding with N atoms of the interface. Because of the limited thickness of amorphous interface, EELS could investigate smaller volume than X-ray absorption spectroscopy (XAS), making it more useful in the interface study.

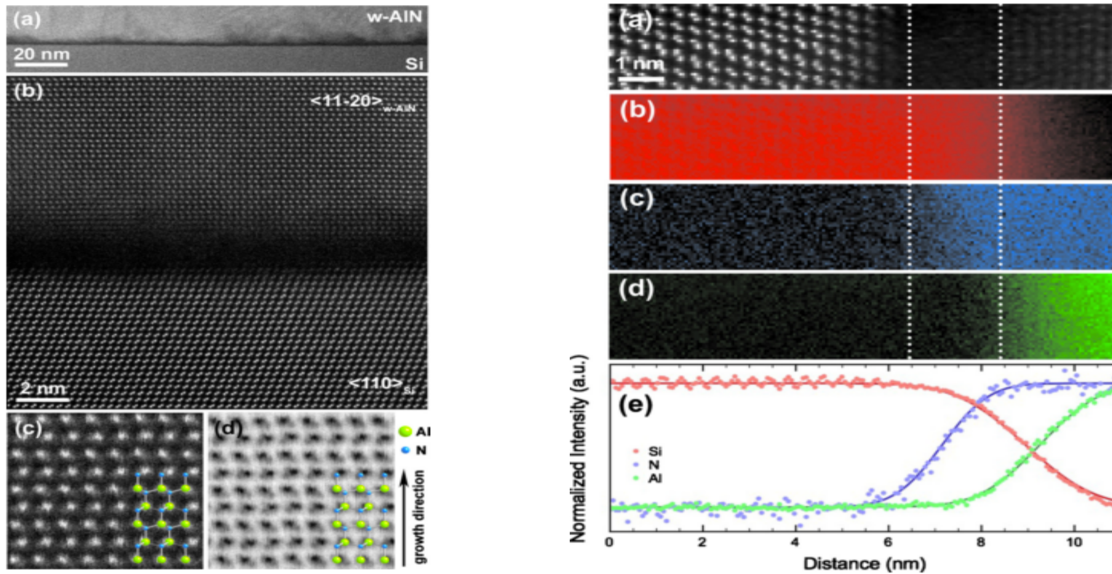

Fig 4. (a, b, c)HAADF image; (d) ABF image;

Fig 5. EELS spectrum-image of the Si<111>/AlN interface(b-Si, c-N, d-Al)

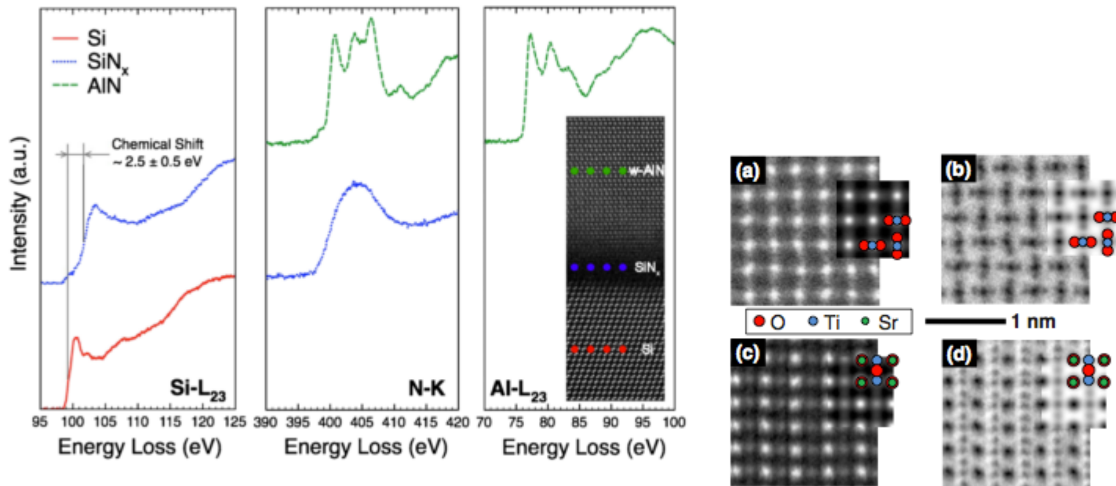

Fig 6 High-energy resolution ELNES obtained from bulk Si (solid line), bulk AlN (dashed line), and from the interfacial layer (dotted line) The spectra displayed here are the sum of spectra acquired by scanning the probe parallel to the interface as indicated by the dots in the inset.

Fig 7 HAADF (left) and ABF(right) images of TiO_2 [001] (a, b) and $SrTiO_3$[110] (c, d).

Insets: Simulations and projected structures

7. Recent Development and Applications:

The improvement of the thermal, vibrational, and acoustical isolation for TEM /STEM, the combination with confocal microscopy, and computer controlled correction of TEM- lens aberrations, as well as relative signal processing & DFT software, make EELS more applicable in many aspects.

The deconvolution techniques, which are based on the Fourier transform, are widely used in the quantitative analysis of EELS data. Besides, we apply statistic methods such as (multiple) least-squares fitting, two-area fitting to separate the spectral components. We could also use multiple-scattering (real space) and density functional calculations to get ELNES. Figure 8 is an example of subtracting background signals, and Figure 9 shows the combination of STEM, EELS, DFT calculations.

The EELS could be applied to the solar cell research. With EELS, we could monitor the growth of the interface, as well as detect the dopant depth concentration (like Boron). And people even apply EELS (phosphorus L_{23}) to the cellular biology, because there is for the ribosome but not for the cytoplasm. Although the spatial resolution is not as good as inorganic systems, it is still practical to localize individual ribosome with different height in a cell. Similarly, we could use nitrogen EELS signals to investigate the total distribution of biomolecules etc.

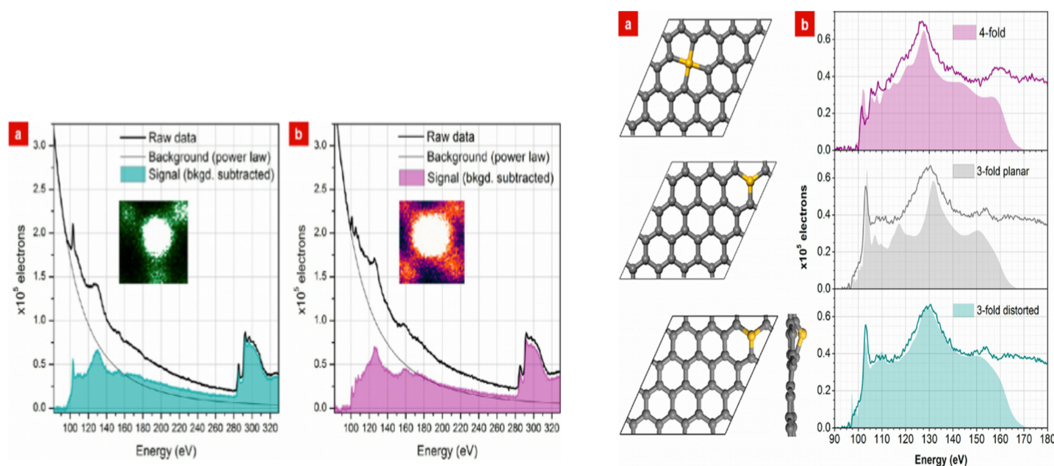

Fig 8 High signal-to-noise EEL spectrum

.Fig 9 (a) Models of Si atoms within a single-layer graphene sheet. The atomic positions were optimized using DFT calculations (b) Comparison between the experimental spectra (solid lines) after background subtraction using a decaying power law, and the spectra calculated by DFT using the models shown in (a) (shaded areas).

8. Epilogue:

After this self-study of electron energy loss spectroscopy (EELS), I gain a better understanding about the instrumentation, physics principles and applications of EELS. I was amazed with various reasons for inelastic scattering, and appreciate the beauty of physics and mathematics when extracting information from the EELS spectrum as well as the delicateness of the instrumental systems. The inspiration of a new experimental technique may occur quite early, but it will take a long way to put it into practice and will become more useful and accurate when combined with other technologies, especially with quantitative analysis and computational methods. EELS will continue to be an important method for qualitatively and quantitatively study for composition, energy bands and bonding, and plasmonic properties of materials, helping us learn more about the nano & micro-scaled world.

Reference:

1. Egerton, R. F. "Electron energy-loss spectroscopy in the TEM." Reports on Progress in Physics 72.1 (2009): 016502.
2. Egerton, Ray F. Electron energy-loss spectroscopy in the electron microscope. Vol. 233. New York: Plenum Press, 1996.
3. Ramasse, Quentin M., et al. "Probing the bonding and electronic structure of single atom dopants in graphene with electron energy loss spectroscopy." Nano letters 13.10 (2013): 4989-4995.
4. Iakoubovskii, K., et al. "Thickness measurements with electron energy loss spectroscopy." Microscopy research and technique 71.8 (2008): 626-631.
5. Rose, H. H. "Optics of high-performance electron microscopes." Science and Technology of Advanced Materials 9.1 (2008): 014107.
6. Findlay, S. D., et al. "Robust atomic resolution imaging of light elements using scanning transmission electron microscopy." Applied Physics Letters 95.19 (2009): 191913.
7. Zewail, Ahmed H. 4D electron microscopy: imaging in space and time. World Scientific, 2010.
8. Willoughby, Arthur. Solar Cell Materials: Developing Technologies. John Wiley & Sons, 2014.
9. Xin, Huolin L., et al. "Scanning Confocal Electron Energy-Loss Microscopy Using Valence-Loss Signals." Microscopy and Microanalysis 19.04 (2013): 1036-1049.
10. Radtke, G., et al. "Scanning transmission electron microscopy investigation of the Si (111)/AlN interface grown by metalorganic vapor phase epitaxy." Applied Physics Letters 97.25 (2010): 251901.